

Manganese phthalocyanine immobilized on silica gel: Efficient and recyclable catalyst for single-step oxidative esterification of aldehydes with alcohols

R.K. Sharma*, Shikha Gulati

Green Chemistry Network Centre, Department of Chemistry, University of Delhi, Delhi 110007, India

ARTICLE INFO

Article history:

Received 8 February 2012

Received in revised form 15 May 2012

Accepted 4 July 2012

Available online 14 July 2012

Keywords:

Silica

Reusable catalyst

Green chemistry

Oxidative esterification

Manganese phthalocyanine

ABSTRACT

The functionalization of silica gel was carried out using 3-aminopropyltriethoxysilane as a reactive surface modifier followed by covalent grafting of novel tetrakis-(2-methoxy-4-formylphenoxy)phthalocyaninato manganese(III) acetate complex. The resulting inorganic–organic hybrid material was found to be a highly selective and recyclable catalyst for the single-step synthesis of esters. The catalyst was characterized by elemental analysis (CHN), diffuse reflectance UV–visible, ^{13}C CPMAS and ^{29}Si CPMAS NMR spectroscopy, X-ray diffraction (XRD), scanning electron microscopy (SEM), BET surface area analysis, energy dispersive X-ray fluorescence (ED-XRF), Fourier-transform infrared (FT-IR) and atomic absorption spectroscopy (AAS) techniques, which demonstrates the covalent grafting of the complex onto functionalized silica gel. The catalytic performance of the novel inorganic–organic hybrid catalyst was evaluated in the direct oxidative esterification of aldehydes with alcohols, at ambient temperature, using hydrogen peroxide as an environment friendly oxidant. The hybrid catalyst presented up to 100% of substrate conversion with high turn-over numbers (TONs), up to 100% of selectivity toward the ester product, and can be recovered and reused for multiple cycles without appreciable loss in its catalytic activity.

© 2012 Elsevier B.V. All rights reserved.

1. Introduction

The ester functionality is present ubiquitously in the structure of significant natural and synthetic molecules; therefore, constitutes an important synthetic target in the pharmaceutical industry, materials science, organic and bioorganic synthesis, etc. [1,2]. Esterification is traditionally a two-step procedure that involves the activation of the carboxylic acid as an acyl halide, anhydride, or activated ester followed by nucleophilic substitution [3,4]. An attractive alternative is the direct catalytic transformation of alcohols or aldehydes to esters under mild conditions, without the use of the corresponding acid or acid derivative [5,6]. Although several catalytic methods have been reported for the direct oxidative esterification of aldehydes, these protocols suffer from numerous drawbacks such as use of large amount of toxic reagents, high temperature, inert atmosphere, long reaction times, photochemical conditions, co-catalyst, or hydrogen acceptors, which render these methods environmentally unsafe and expensive [7–15]. Moreover, the recovery of catalyst from the reaction mixture is another one of the major drawbacks as the process of extracting the catalyst can often destroy it.

In today's milieu, one of the challenging issues for chemists is to pursue green chemical transformations [16,17]. Because of

the huge amount of toxic wastes and byproducts arising from chemical processes, chemists have been constrained to develop cost-effective and environmentally friendly catalytic routes that minimize waste. In this context, direct oxidative esterification of aldehydes with alcohols using environmentally benign oxidant, i.e. hydrogen peroxide in the presence of reusable heterogeneous catalyst under mild conditions is a facile, cost-effective, and environmentally friendly procedure that avoids the use of expensive activators and excess of reagents.

Metallophthalocyanines (MPcs) are very well known to catalyze a variety of oxidative transformations [18–21]. The driving forces for the catalytic use of phthalocyanines are (i) their economical and facile preparation in a large scale; (ii) the structure analogy with that of porphyrins, which are widely used by nature in the active sites of oxygenase enzymes; (iii) their chemical and thermal stability [22]. Despite the various advantages, their separation from the reaction media is the main drawback from the viewpoint of the application in catalysis. This problem can be overcome by the immobilization of MPcs on solid supports in order to make catalysts recoverable and reusable. Recently, we have reported the oxidative bromination reaction using Cu^{2+} -perfluorophthalocyanine-immobilized silica gel catalyst under mild reaction conditions [23]. Different methodologies can be used to immobilize the complexes onto support materials [24–27]. But, covalent immobilization of catalysts on inorganic supports is highly effective since it maintains the inherent activity and selectivity of the catalytic center [28]. Among various inorganic

* Corresponding author. Tel.: +91 011 27666250; fax: +91 011 27666250.
E-mail address: rksharmagreenchem@hotmail.com (R.K. Sharma).

supports, silica gel is very advantageous since it possesses high surface area, good thermal and mechanical stability, easy availability and inexpensiveness, and relatively simple covalent modification with organic or organometallic moieties [29].

Thus, considering the above advantages and in continuation of our research work on designing recyclable heterogeneous catalytic systems [30–36] for various organic transformations, herein we report the single-step oxidative esterification of aldehydes with alcohols in presence of newly synthesized tetrakis-(2-methoxy-4-formylphenoxy)phthalocyaninato manganese(III) acetate complex immobilized on silica gel as recyclable catalyst using hydrogen peroxide as an oxidant.

2. Experimental

2.1. Materials and instruments

N,N-dimethylaminoethanol (DMAE) (98%) was obtained from Fluka and used as such in this study. 3-Aminopropyltriethoxysilane (APTES) (98%), silica gel (60–100 mesh, according to the supplier specifications), and H₂O₂ solution (30 wt.% in water) were obtained from Sigma–Aldrich. Starting materials and reagents used in the reactions were obtained commercially from Spectrochem. Pvt. Ltd., India and used as such in this study. The Fourier transform infrared (FT-IR) spectra of the compounds were obtained on a Perkin-Elmer spectrometer at room temperature using KBr pellet technique in the range of 4000–400 cm⁻¹ under the atmospheric conditions with a resolution of 1 cm⁻¹. Solid-state ¹³C and ²⁹Si cross-polarization magic-angle spinning (CPMAS) NMR spectra were recorded on Bruker DSX-300 NMR spectrometer. Powder X-ray diffraction (XRD) patterns of the samples were obtained on a Bruker D8 ADVANCE X-ray diffractometer using graphite monochromatized Cu-K α radiation. Specific surface area was calculated using the BET method on Gemini-V2.00 instrument (Micromeritics Instrument Corp.). Samples were outgassed at 100 °C for 3 h to evacuate the physically adsorbed moisture before measurement. The diffuse reflectance UV–visible spectrum of the catalyst was obtained over the spectral range of 300–800 nm in the BaSO₄ phase using Perkin-Elmer Lambda 35 scanning double beam spectrometer equipped with a 50 mm integrating sphere. Elemental analysis (CHN) was performed using Elementar Analysensysteme GmbH VarioEL V3.00 instrument. The amount of manganese in the catalyst (MnPc–APSG) and the filtrate was estimated by atomic absorption spectroscopy (AAS) on LABINDIA AA 7000 Atomic Absorption Spectrometer using an acetylene flame. The optimum parameters for Mn measurements are: wavelength = 279.50 nm; lamp current = 3 mA; slit width = 0.2 nm; fuel flow rate = 0.2 L min⁻¹. Energy dispersive X-ray fluorescence spectroscopy was performed on Fischerscope X-Ray XAN-FAD BC. Scanning electron microscopy (SEM) images were obtained using a ZEISS EVO 40 instrument. The samples were placed on a copper tape and then coated with a thin layer of gold using a sputter coater. The products obtained were analyzed and confirmed on Agilent gas chromatography (6850 GC) and a quadrupole mass filter equipped 5975 mass selective detector (MSD) using helium as carrier gas (rate 0.9 ml min⁻¹).

2.2. Catalyst preparation

2.2.1. Preparation of tetrakis-(2-methoxy-4-formylphenoxy)phthalocyaninato manganese(III) acetate (MnPc)

The phthalocyanine precursor, i.e. 4-(2-methoxy-4-formylphenoxy)phthalonitrile was prepared according to the reported protocol [37] with slight modification (Supplementary material). To prepare tetrakis-(2-methoxy-4-formylphenoxy)phthalocyaninato manganese(III) acetate [38],

a mixture of manganese acetate (0.77 mmol, 0.206 g), 4-(2-methoxy-4-formylphenoxy)phthalonitrile (18.5 mmol, 5.14 g), N,N-dimethylaminoethanol (DMAE) (5 ml) and DBU (1 mL) were irradiated in microwave reactor at 370 W for 10 min. After cooling to room temperature the solution was poured into methanol/water (3:1) and centrifuged. The precipitated solid was filtered off, washed with methanol/water mixture and dried under vacuum oven. Yield: 75%; Melting point: >200 °C; Anal. Calc. for C₆₆H₄₃MnN₈O₁₄ (Mol. wt. = 1227.03): C 64.60, H 3.53, N 9.13, Mn 4.48; Found C 64.68, H 3.48, N 9.14, Mn 4.52; IR ν (cm⁻¹): 1617 (aromatic C=C), 1320 (aromatic C=N stretching), 1113 (C–O–C), 493 (Mn–N); UV-visible (N-methyl-2-pyrrolidinone), λ_{max} (nm): 671, 689.

2.2.2. Preparation of silica supported manganese(II) phthalocyanine (MnPc–APSG)

Firstly, silica gel (SG) was functionalized using 3-aminopropyltriethoxysilane (APTES) to give aminopropyl-functionalized silica gel (APSG) according to a greener protocol [39]. 1 mL of 3-APTES was dissolved in 100 mL of distilled water acidified with acetic acid (pH = 4). Then, 2 g of activated silica gel (dried in oven at 150 °C for 18 h) was added in the silane solution and stirred for 2 h at room temperature. The product was filtered off and kept in oven at 150 °C for 4 h. The dried product was washed consecutively with water, ethanol and acetone several times to remove the un-grafted material and dried for another 2 h at 120 °C. Then, a mixture of APSG (5 g) and MnPc (1 mmol) in N,N-dimethylaminoethanol was refluxed for 4 h (Scheme 1). The resulting inorganic–organic hybrid material (MnPc–APSG) was filtered, washed with water and dried in vacuum oven.

2.3. Catalytic reaction

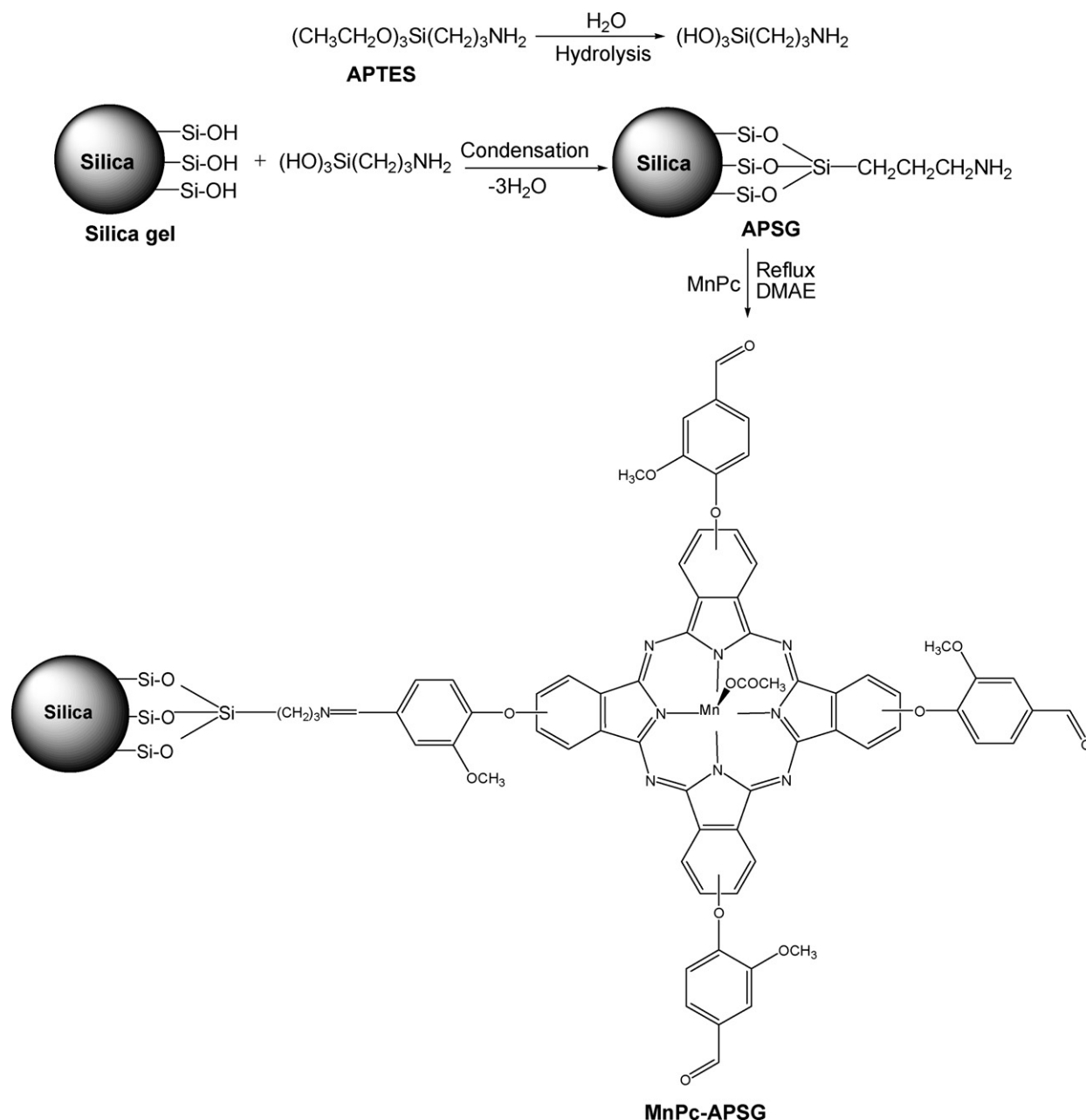
The catalytic reactions were performed in a round-bottomed flask equipped with a magnetic stirring bar and a reflux condenser. The oxidative esterification was carried out as follows: catalyst (20 mg), aldehyde (1 mmol) and alcohol (5 mmol) were magnetically stirred in the reaction flask at 60 °C. H₂O₂ (2 mmol) was progressively added to the reaction mixture using a syringe. The reactions were stopped after 3 h and the excess hydrogen peroxide was deactivated by the addition of aq. sodium bisulfite. The catalyst was separated from the reaction mixture by filtration. As a two-layer mixture was obtained (organic phase/water phase) after the reaction, the organic products were separated from the aqueous phase by ethyl acetate extractions. The combined organic layers were washed with brine and dried over anhydrous Na₂SO₄, and then analyzed by GC–MS.

3. Results and discussion

3.1. Catalyst characterization

3.1.1. FT-IR spectroscopy

The FT-IR spectroscopy is usually employed to monitor the immobilization process by comparing the precursor and modified surfaces (Supplementary material). The spectra of the silica gel (SG) and APSG showed bands characteristic of the support matrixes which are assigned to surface hydroxyl groups, in the range of 3770–3300 cm⁻¹, and to lattice vibrations, in the range of 1300–750 cm⁻¹. In case of silica gel, peak at 800 cm⁻¹ is assigned to silanol group. No major changes are observed in the silica gel structure sensitive vibrations, after the reaction of APTES modifier with the surface –OH groups, which indicate that its framework remained unaffected. The spectrum of APSG exhibits an extra band at about 2926 cm⁻¹ due to the aliphatic (–CH₂) stretching of the propyl chain of the silylating agent [40–42] and the peak due to



Scheme 1. Preparation of silica supported manganese phthalocyanine catalyst (MnPc-APSG).

silanol groups has disappeared confirming that silica gel surface was functionalized with APTES. Furthermore, moving from silica gel to APSG, a significant reduction of the intensity of the O–H stretching and bending vibrations bands and of the peak from Si–OH stretching modes is observed. The peak around 1633 cm^{-1} corresponds to N–H bending vibration of $-\text{NH}_2$ groups, which is overlapped by the bending vibration of adsorbed H_2O . In case of catalyst, the IR bands related to the anchored complex are very weak when compared to those associated with the support and grafted APTES, due to the low complex loading. By comparing the spectra of APSG with those of catalyst (MnPc-APSG), it is observed that after the Schiff condensation reaction, the characteristic band of the imine group ($\text{C}=\text{N}$) appears in the spectrum of MnPc-APSG at 1638 cm^{-1} slightly shifted from a matrix band confirming that MnPc is successfully anchored onto the surface of silica gel. In case of recycled catalyst, none of the vibrations change significantly compared to fresh MnPc-APSG. This suggests existence of all the

properties in recycled catalyst compared to fresh heterogeneous catalyst.

3.1.2. ^{13}C CP-MAS and ^{29}Si CP-MAS NMR studies

The conservation of 3-aminopropyl group after functionalization of silica gel is confirmed by solid state ^{13}C NMR spectroscopy. The ^{13}C CPMAS NMR spectrum of aminopropylated silica gel (APSG) shows the presence of three well resolved peaks at 9.3, 22.3 and 42.9 ppm assigned to C1, C2, and C3 carbons of the incorporated aminopropyl group- $\text{O}_3\text{SiCH}_2(1)\text{CH}_2(2)\text{CH}_2(3)\text{NH}_2$, respectively (Fig. 1(a)) which authenticate the synthesis of APSG [43,44]. The covalent linkage between the silanol groups and the organic moiety on the silica can also be established by means of ^{29}Si CPMAS NMR spectroscopy. The solid-state ^{29}Si NMR spectrum of MnPc-APSG shows four peaks (Fig. 1b): -58 ppm assigned to Si–OH of $\text{C}-\text{Si}(\text{OSi})_2(\text{OH})$ group (T^2) and -67 ppm assigned to $\text{C}-\text{Si}(\text{OSi})_3$ group (T^3), which provides direct evidence that the hybrid catalyst

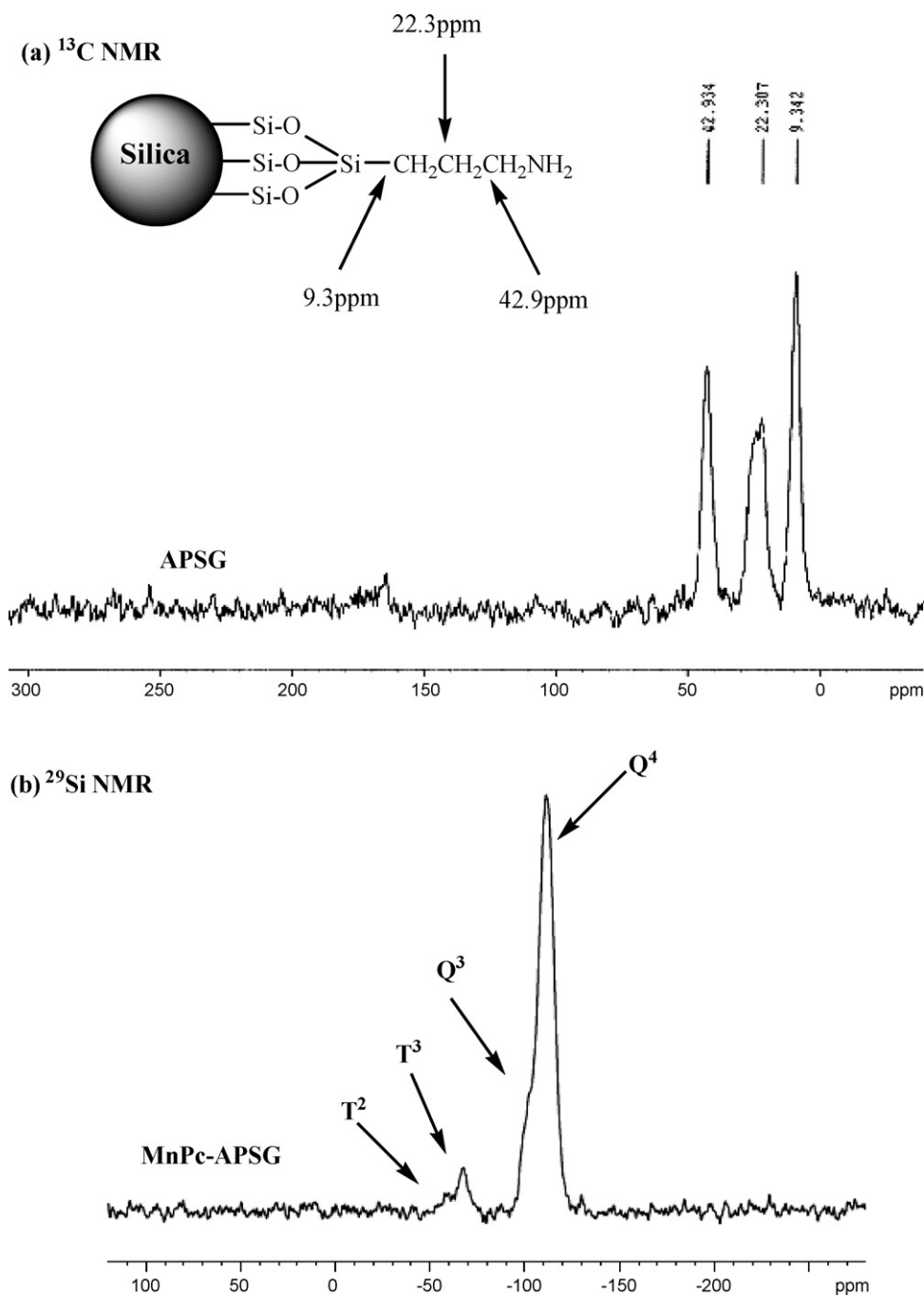


Fig. 1. (a) ^{13}C CPMAS NMR spectrum of APSG and (b) ^{29}Si CP-MAS NMR spectrum of MnPc-APSG catalyst.

(MnPc-APSG) consists of a highly condensed siloxane network with an organic group covalently bonded to the silica gel. Two other typical peaks correspond to the inorganic polymeric structure of silica: -111 ppm assigned to $\text{Si}(\text{OSi})_4$ group (Q^4) and -101 ppm assigned to the free silanol group of $\text{Si}(\text{OSi})_3\text{OH}$ (Q^3) [45–48].

3.1.3. BET surface area and elemental analysis

A high-quality distribution of active species over a high surface area support material is generally enviable for superior catalytic activity. Actually, the anchoring of organic or organometallic moieties onto the silica matrix blocks the access of nitrogen gas molecules thereby reducing its surface area. Hence, as expected, the BET surface area decreased after grafting [49–51], according

to the following sequence $\text{SG} > \text{APSG} > \text{MnPc-APSG}$ (Table 1). The reduction in surface area in this sequence confirms the functionalization of silica gel with 3-aminopropyltriethoxy silane to give APSG, and its modification with MnPc to yield MnPc-APSG.

Table 1
Physico-chemical parameters of silica gel (SG), aminopropyl silica gel (APSG) and catalyst (MnPc-APSG).

Material	Elemental analysis			BET surface area (m^2/g)
	%C	%H	%N	
SG	–	–	–	235
APSG	2.94	1.64	1.09	174
MnPc-APSG	28.42	9.82	4.06	152

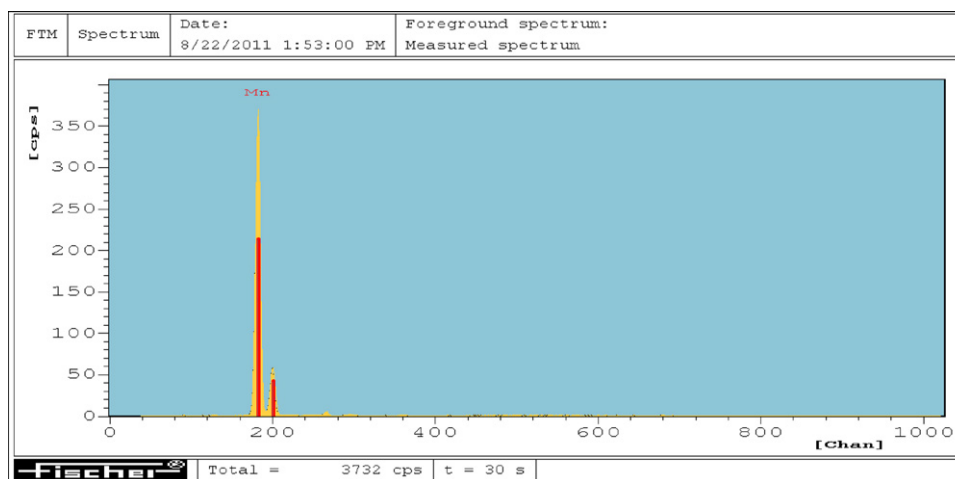


Fig. 2. ED-XRF spectrum of MnPc-APSG catalyst.

The ninhydrin test (Supplementary material) was performed to detect qualitatively the existence of free amine species on APSG [52]. The color of the material changed from white to blue when the ninhydrin solution was added, confirming the presence of free amine groups. In contrast, the test was negative for the parent silica gel (no color change).

The chemical composition of the organo-functional groups covalently anchored on silica gel is determined by elemental analyses (Table 1). The elemental analysis of APSG leads to the appearance of nitrogen (1.09%) as well as the carbon surface content (2.94%), providing an evidence for the APTES immobilization onto silica gel. The observed carbon and nitrogen contents of APSG shows C/N ratio to be ~ 2.5 which is close to the expected value thereby confirming the 3-APTES grafting onto the surface of silica gel. The nitrogen loading of APSG is 0.77 mmol g^{-1} , which corresponds to APTES functionalization efficiency of 36% (estimated by the expression: amount of grafted APTES/amount used in the functionalization reaction $\times 100$). The presence of well resolved peak of manganese is observed in the ED-XRF spectrum (Fig. 2) of the MnPc-APSG which confirms the immobilization of manganese phthalocyanine complex (MnPc) on the modified silica gel. The chemical analyses of MnPc-APSG catalyst (Table 1) revealed the presence of organic matter with a C/N ratio roughly similar to that of phthalocyanine. Further to support the successful immobilization, and in order to quantify the amount of manganese in the MnPc-APSG it was digested in nitric acid and then subjected to AAS determination which gives 0.175 mmol of Mn per gram of catalyst, which corresponds to an anchoring efficiency (amount of anchored complex/amount in original solution $\times 100$) of 87.5%. This value suggests that catalyst has free $-\text{NH}_2$ groups as well.

3.1.4. Powder X-ray diffraction studies

X-ray diffraction (XRD) analysis is carried out to investigate the structure of silica gel, APSG and MnPc-APSG. The diffractograms of these materials (Fig. 3) shows that all the materials are amorphous or non-periodic. The broad peak centered around $2\theta = 23^\circ$ in the XRD patterns of silica gel, APSG and MnPc-APSG is ascribed to the diffraction peak of amorphous silica, which clearly depicts that there is no change in the topological structure of silica gel before and after grafting reactions [53]. However, after organo-functionalization and metal complex loading there is a slight decrease in intensity [54] with broadening of corresponding peak indicating a slight disorder in the APSG and MnPc-APSG. The XRD pattern of reused MnPc-APSG (Supplementary material) also gives diffraction peak of amorphous silica.

3.1.5. Diffuse reflectance UV-visible spectroscopy

MnPc-APSG is prepared by Schiff condensation reaction of carbonyl group of manganese phthalocyanine complex with the $-\text{NH}_2$ groups of APSG. Thus, the covalent grafting of MnPc complex on APSG is confirmed by diffuse reflectance UV-visible spectroscopy. The diffuse reflectance UV-vis spectrum of silica gel does not have any absorption band in the region of 300–900 nm. On the other hand, the diffuse reflectance UV-visible spectrum of MnPc-APSG (shown in Fig. 4) exhibits broad absorption band in the region of 550–800 nm due to ligand $\pi-\pi^*$ electronic transitions, confirming that MnPc complex has covalently anchored on APSG without degradation. The blue shift is observed which is indicative of an increased π overlap on immobilization of manganese phthalocyanine complex [55].

3.1.6. Scanning electron microscopy (SEM)

MnPc-APSG presents the same morphology (Fig. 5(a)) as that of parent silica gel (Fig. 5(b)). Moreover, no clog occurred between silica particles during the preparation of catalyst, and the particles maintained regular lumpy shape. It could be seen that the particles appearance and its size are very similar, demonstrating that the particles of silica gel had good mechanical stability, and they had not been destroyed during the whole surface modification reaction [29].

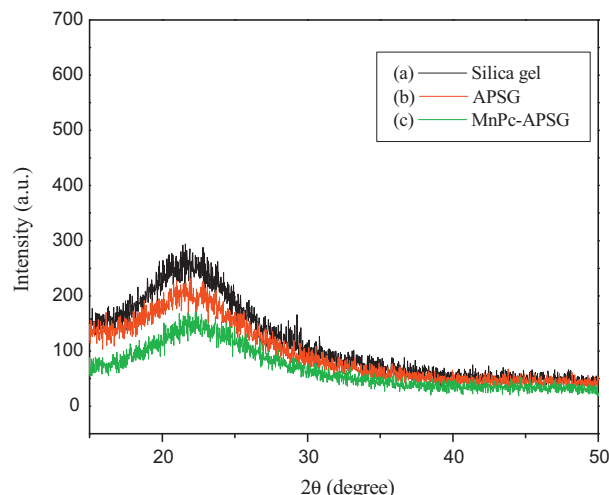


Fig. 3. XRD pattern of (a) silica gel, (b) APSG and (c) MnPc-APSG.

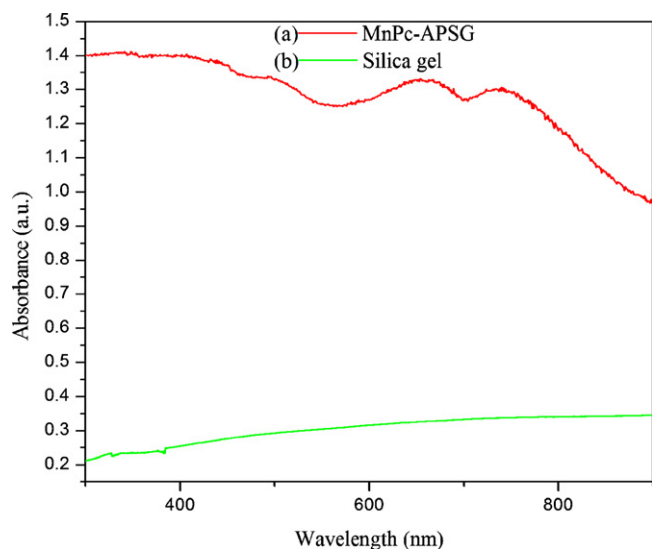


Fig. 4. Diffuse reflectance UV-visible spectra of (a) catalyst (MnPc-APSG) and (b) silica gel.

3.2. Catalytic activity of MnPc-APSG

In order to examine the effects of catalyst on the direct transformation of aldehydes to corresponding esters, benzaldehyde and methanol were chosen as test substrates to react in the presence of hydrogen peroxide as oxidant. The use of MnPc catalyst gave lower conversion than heterogenized MnPc (Table 2). The use of simple metal salt (manganese acetate) as catalyst showed quite poor activity pointing out the importance of the phthalocyanine ring. In addition, these homogeneous catalysts decomposed after the

Table 2
Oxidative esterification of benzaldehyde with methanol using various catalysts.^a

Entry	Catalyst	Time (h)	Conv. ^b (%)	TON (TOF) ^c
1	^d Mn(OAc) ₂	3	75	250 (83)
2	^d MPc	3	88	293 (97)
3	MPc-APSG	3	100	333 (111)
4	SG	5	5	–
5	No catalyst	8	1	–
6	^e MPc-APSG	4	55	183 (45)

^a Reaction conditions: catalyst (20 mg), benzaldehyde (1 mmol), methanol (5 mmol) and 30% H₂O₂ (2 mmol) at 60 °C.

^b Conversion was determined by GC.

^c TON is the number of moles of product per mole of catalyst and TOF = TON per hour.

^d 0.003 mmol.

^e Reaction conditions: catalyst (20 mg), benzaldehyde (1 mmol), methanol (5 mmol), aerobic conditions at 60 °C.

reaction and could not be reused. The results indicated that the direct transformation of benzaldehyde with methanol in the presence of catalyst were faster than without using catalyst. MnPc-APSG catalyst was also found to work under aerobic conditions but low conversion rate was observed (Scheme 2).

In order to understand the scope and generality of the reaction, a wide range of aldehydes (aromatic, aliphatic & allylic) was subjected to the reaction with a variety of alcohols under these reaction conditions (Table 3). As can be seen, the catalytic system worked exceedingly well in case of aromatic aldehydes with both electron-rich and electron-withdrawing groups. Other alcohols could be substituted for methanol to provide corresponding esters. With this end in view, the reaction was performed in the presence of ethyl alcohol under identical conditions as described for methyl esters. Thus, various ethyl esters can be prepared efficiently by the present methodology as shown in Table 3. The success

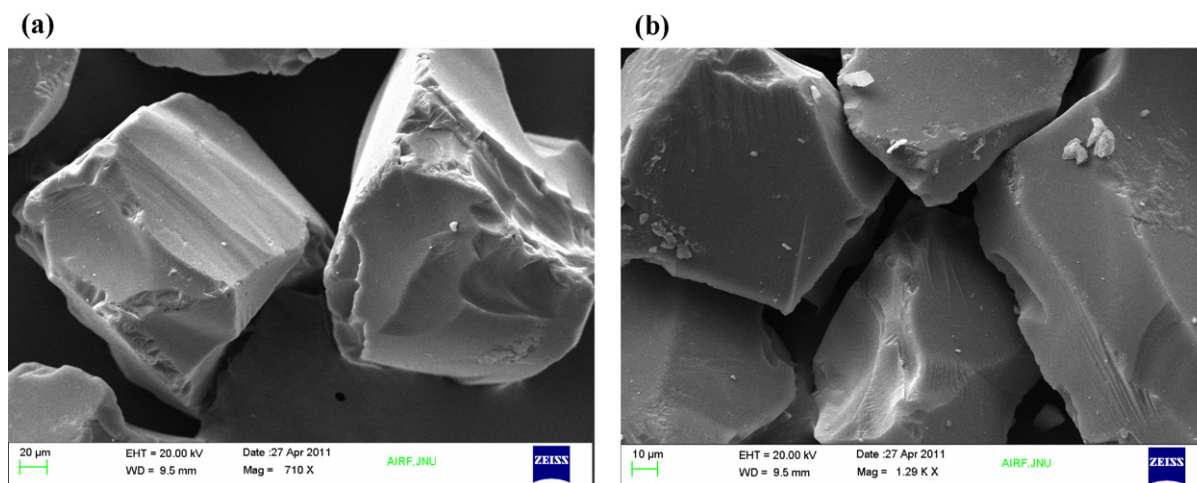
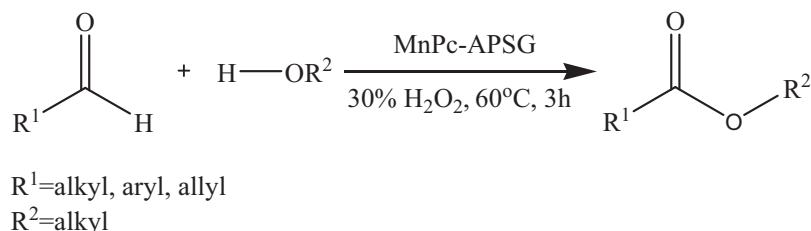


Fig. 5. SEM images of (a) silica gel and (b) MnPc-APSG catalyst.



Scheme 2. Silica supported manganese phthalocyanine (MnPc-APSG) catalyzed oxidative esterification of aldehydes with alcohols to corresponding esters.

Table 3
MnPC–APSG catalyzed oxidative esterification of aldehydes with alcohols.^a

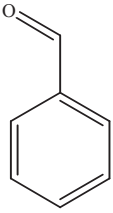
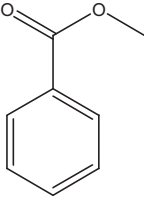
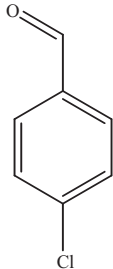
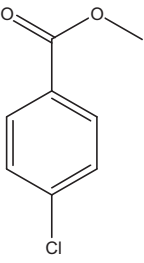
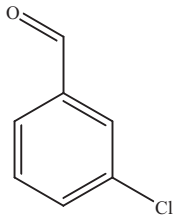
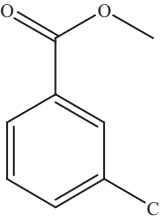
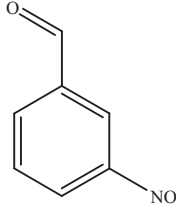
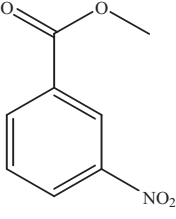
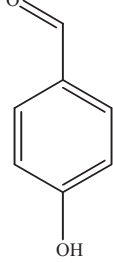
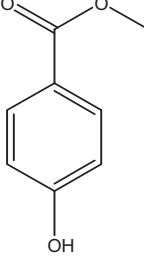
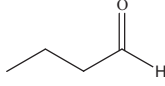
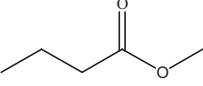
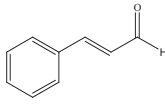
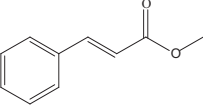
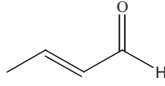
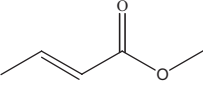
Entry	Aldehyde	Alcohol	Product	Conv. ^b (%)	TON (TOF) ^c	Selectivity ^d (%)
1		HO—CH ₃		100	333 (111)	100
2		HO—CH ₃		98	326 (108)	97
3		HO—CH ₃		95	316 (105)	95
4		HO—CH ₃		96	320 (106)	94
5		HO—CH ₃		98	326 (108)	100
6		HO—CH ₃		91	303 (101)	90
7		HO—CH ₃		72	240 (80)	68
8		HO—CH ₃		64	213 (71)	59

Table 3 (Continued)

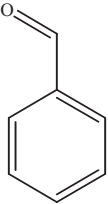
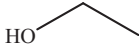
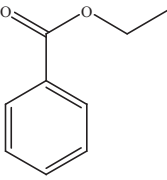
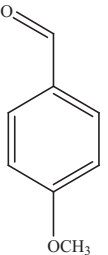
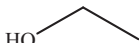
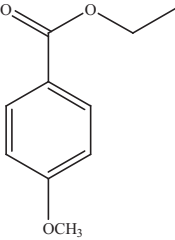
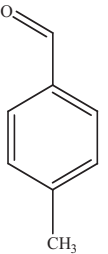
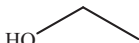
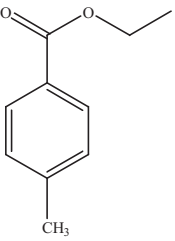
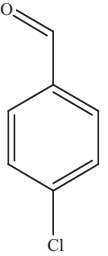
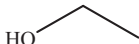
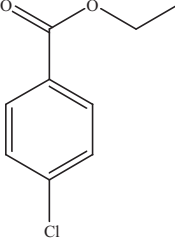
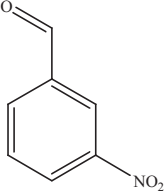
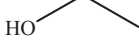
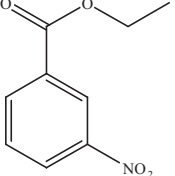
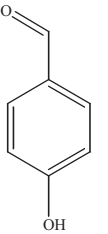
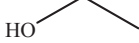
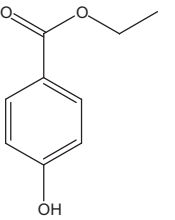
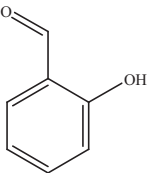

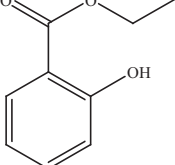
Entry	Aldehyde	Alcohol	Product	Conv. ^b (%)	TON (TOF) ^c	Selectivity ^d (%)
9				100	333 (111)	98
10				98	326 (108)	97
11				100	333 (111)	>99
12				92	306 (102)	95
13				94	313 (104)	96
14				100	333 (111)	95
15				99	330 (110)	93

Table 3 (Continued)

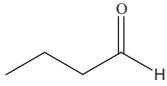
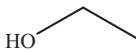
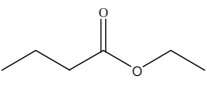
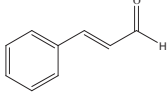
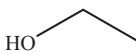
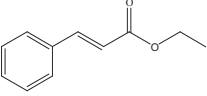
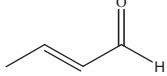
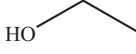
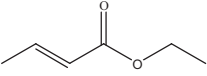
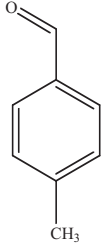
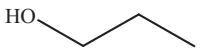
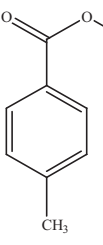
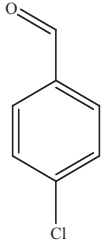
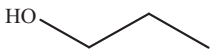
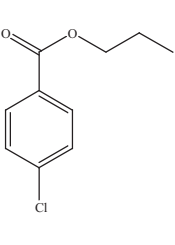
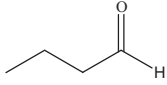
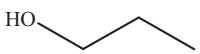
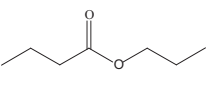
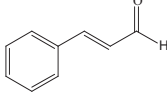
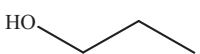
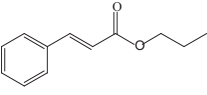
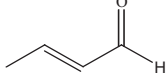
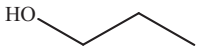
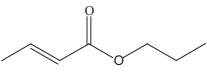
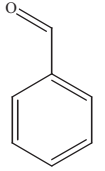
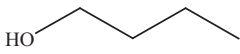
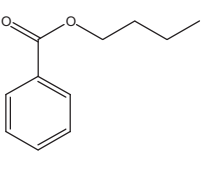
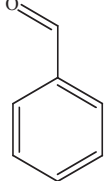
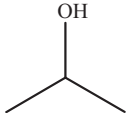
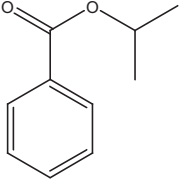
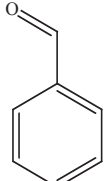
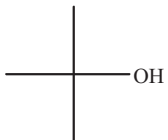
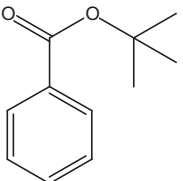
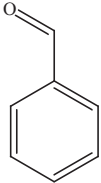
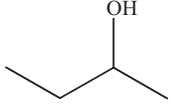
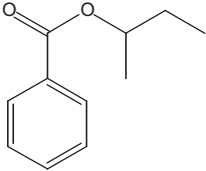
Entry	Aldehyde	Alcohol	Product	Conv. ^b (%)	TON (TOF) ^c	Selectivity ^d (%)
16				85	283 (94)	88
17				65	216 (72)	64
18				58	193 (64)	45
19				88	293 (97)	95
20				85	283 (94)	95
21				78	260 (86)	82
22				58	193 (64)	65
23				51	170 (56)	34
24				60	200 (66)	-
25				20	66 (22)	-
26				5	16 (5)	-

Table 3 (Continued)

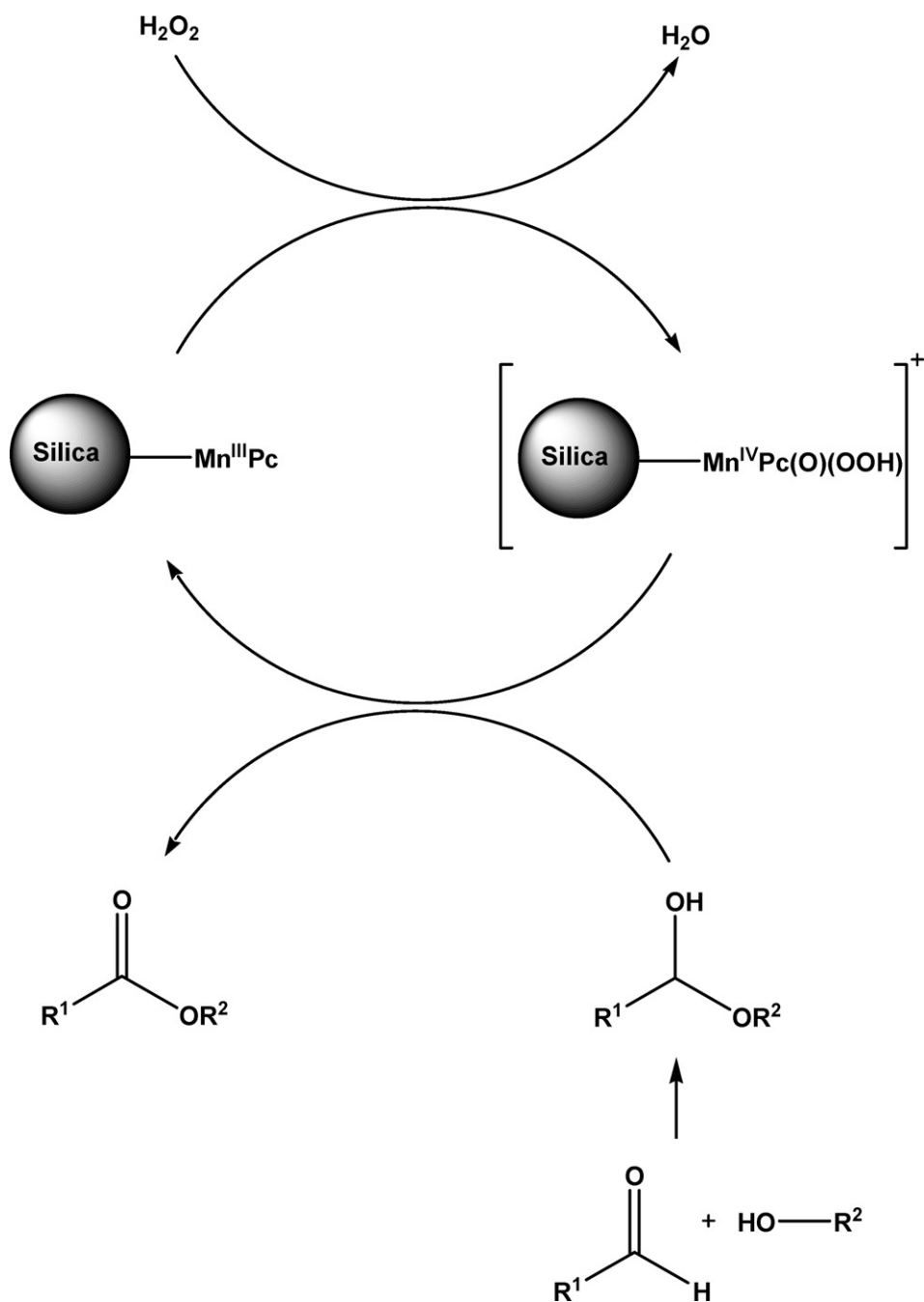
Entry	Aldehyde	Alcohol	Product	Conv. ^b (%)	TON (TOF) ^c	Selectivity ^d (%)
27				2	6 (2)	–

^a Reaction conditions: catalyst (20 mg), aldehyde (1 mmol) alcohol (5 mmol) and 30% H₂O₂ (2 mmol), reflux at 60 °C for 3 h.

^b Conversion and selectivity were determined by GC.

^c TON is the number of moles of product per mol of catalyst and TOF = TON per hour.

^d Selectivity of the ester was measured based on the aldehyde conversion.



Scheme 3. Plausible rationale for oxidative esterification of aldehydes with alcohols.

Table 4
Literature precedents of metal-catalyzed oxidative esterification reaction.

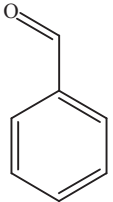
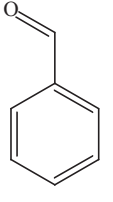
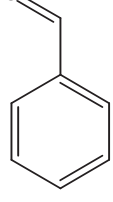
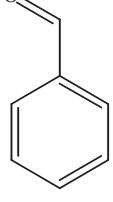
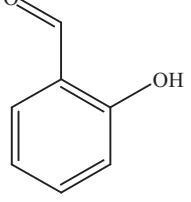
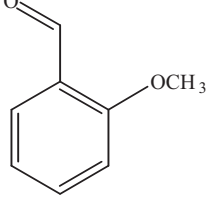
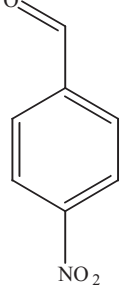
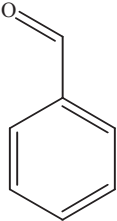
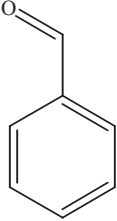
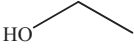
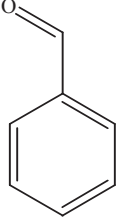
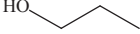
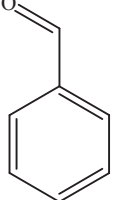
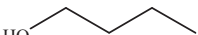
Entry	Aldehyde	Alcohol	Catalytic conditions	Time (h)	Conv. (%)	Selectivity (%)	Ref.
1		HO—CH ₃	Au/ β -Ga ₂ O ₃ , 90 °C, 5 atm O ₂	1	99	94.3	[56]
2		HO—CH ₂ —CH ₃	Au/ β -Ga ₂ O ₃ , 90 °C, 5 atm O ₂	3	92	95	[56]
3		HO—CH ₂ —CH ₂ —CH ₃	Au/ β -Ga ₂ O ₃ , 90 °C, 5 atm O ₂	2	95	95.8	[56]
4		HO—CH ₃	Pd ₅ Pb ₅ Mg ₂ /Al ₂ O ₃ , 80 °C, NaOH, Mg(OH) ₂ 6.0–8.0 pH value	2	80.1	66.4	[57]
5		HO—CH ₃	V ₂ O ₅ –H ₂ O ₂	7.5	93	100	[9]
6		HO—CH ₃	V ₂ O ₅ –H ₂ O ₂	5	100	91	[9]
7		HO—CH ₃	KI, H ₂ O ₂ , 65 °C	21	6	95	[58]

Table 4 (Continued)

Entry	Aldehyde	Alcohol	Catalytic conditions	Time (h)	Conv. (%)	Selectivity (%)	Ref.
8		HO—CH ₃	Au/TiO ₂ , O ₂ , NaOMe	4	100	100	[59]
9			Au/TiO ₂ , O ₂ , NaOMe	20	90	100	[59]
10			Au/TiO ₂ , O ₂ , NaOMe	20	95	100	[59]
11			Au/TiO ₂ , O ₂ , NaOMe	20	60	100	[59]

of this methodology was further demonstrated by oxidative esterification of benzaldehyde with other alcohols such as 1-propanol, which also gave high conversions. However, esters of branched alcohols such as 2-propanol, 2-butanol and tert-butyl alcohol could not be obtained, which could be due to an unfavorable equilibrium in hemiacetal formation due to the steric strain. More satisfying was the compatibility of the reaction to proceed successfully with aliphatic aldehydes also, however, allylic aldehydes showed lower conversion and selectivity.

Table 4 presents the literature precedents of metal catalyzed oxidative esterification of aldehydes with alcohols under different reaction conditions and the results have been compared with those obtained by using MnPc-APSG as catalyst (Table 3). It is evident from the comparison of the two tables that conversion and selectivity of substrates obtained from the inorganic-organic hybrid catalyst (MnPc-APSG) are far better than those obtained by some other reported heterogeneous catalysts.

Possible mechanism of the reaction is shown in Scheme 3. Transition metal catalyzed oxidative esterification is expected to be versatile procedure directly giving esters from aldehyde and alcohol via formation of hemiacetal intermediate. The only viable mechanism to explain the dominant catalytic process is the Lewis acid pathway in which oxygen atom is first transferred to the Mn(III) species (catalyst) from the hydrogen peroxide (oxidant) to form a high oxidation state Mn(IV)-oxo species which will further facilitates the oxidation of hemiacetal to generate the corresponding ester [60].

3.3. Reusability and heterogeneity test

The reusability of a catalyst is of great importance in consideration of industrial application, and therefore, is one of the prior factors being considered in catalyst design. To address the issue, a series of tests were undertaken. To test the leaching of the MnPc-complex from the silica support, 'filtration method' was carried out. Accordingly, in a typical catalytic oxidative esterification of benzaldehyde with methanol, after 2 h, the solid catalyst was filtered. The progress of the reaction in the filtrate was monitored by GC. The data showed that, no further increase in conversion in the filtrate after 5 h (Table 5). The filtrate was digested in nitric acid (5 mL) in a microwave digester system for 10 min. The volume of the samples was then adjusted to 25 mL using deionized water. Reference solutions of manganese with high degree of analytical purity were used to obtain the calibration curves. The investigation of the

Table 5

Conversion for oxidative esterification of benzaldehyde under optimized conditions (with and without catalyst).

Entry	Time (h)	Conversion (%)	Selectivity (%)
1 ^a	2	78	100
2 ^b	5	78	100

^a Reaction conditions: catalyst (20 mg), benzaldehyde (1 mmol), methanol (5 mmol) and 30% H₂O₂ (2 mmol), reflux at 60 °C for 3 h.

^b Filtrate after the removal of catalyst (please refer Section 3.3. in the text for more details).

Table 6Catalytic reusability test for oxidative esterification of benzaldehyde with methanol.^a

Run	Conversion ^b (%)	Selectivity (%)
Fresh	100	100
1	100	100
2	100	>99
3	100	>99
4	98	>99
5	98	>99
6	97	>99

^a Reaction conditions: catalyst (20 mg), benzaldehyde (1 mmol), methanol (5 mmol) and 30% H₂O₂ (2 mmol), reflux at 60 °C for 3 h.^b Conversion and selectivity were determined by GC.

resulting solution by atomic absorption method showed no detectable (<0.01 ppm) manganese. The manganese content was quantified in duplicate for each sample. This ensured that no leaching of the active supported MnPc-complex occurred. Thus, the obtained catalytic results derive exclusively from the heterogeneous catalyst. It is noteworthy that the work-up of the reaction mixture is rather simple since the catalyst can be recovered by simple filtration. The recovered catalyst is capable of being reused in subsequent cycles after washing with ethyl acetate and water. The conversion of the aldehyde after six cycles was almost constant and no loss of catalytic activity and selectivity was observed compared with the fresh catalyst. The results obtained by recycling of the catalyst are shown in Table 6. The recycling result suggests heterogeneity of the catalyst. The reused catalyst was also subjected to XRD and FT-IR spectroscopy (Supplementary material). Comparison of IR spectra and XRD patterns of fresh and recovered catalysts depicts that the structural properties of the anchored complex remains unaltered after the oxidative esterification reaction.

4. Conclusion

We have developed an environmentally benign protocol for the highly selective oxidative esterification of aldehydes with alcohols catalyzed by silica supported manganese catalyst using hydrogen peroxide, an environment friendly oxidant. Catalyst/product separation is very simple and the catalyst recovered after the reaction is reusable as it retains its catalytic performance. Because of its high recyclability and the use of hydrogen peroxide as the oxidant, this protocol has environmental and economic advantages over other supported catalytic systems. In addition, the advantages of this catalytic system also includes high substrate conversion, short reaction time, ambient temperature, mild reaction conditions, high catalytic turnover number which make it a greener alternative for the direct synthesis of esters from aldehydes.

Acknowledgement

The financial assistance from University Grant Commission and DU-DST PURSE grant is acknowledged. Due thanks to AIRF, JNU, Delhi, India for SEM analysis and IISc, Bangalore, India for solid state NMR measurements.

Appendix A. Supplementary data

Supplementary data associated with this article can be found, in the online version, at <http://dx.doi.org/10.1016/j.molcata.2012.07.004>.

References

- [1] E.J. Corey, N.W. Gilman, B.E. Ganem, *J. Am. Chem. Soc.* 90 (1968) 5616–5617.
- [2] R. Gopinath, A.R. Paital, B.K. Patel, *Tetrahedron Lett.* 43 (2002) 5123–5126.

- [3] J. Otera, *Esterification: Methods, Reactions and Applications*, Wiley, New York, 2003.
- [4] R.C. Larock, *Comprehensive Organic Transformations*, VCH, New York, 1989.
- [5] K.E. Kovi, C. Wolf, *Chem. Eur. J.* 14 (2008) 6302–6315.
- [6] H. Miyamura, T. Yasukawa, S. Kobayashi, *Green Chem.* 12 (2010) 776–778.
- [7] B.S. Bal, Y.W. Childers, H.W. Pinnick, *Tetrahedron* 11 (1980) 2091–2096.
- [8] M. Okimoto, T. Chiba, *J. Org. Chem.* 53 (1987) 218–220.
- [9] R. Gopinath, B.K. Patel, *Org. Lett.* 2 (2000) 577–579.
- [10] B.R. Travis, M. Sivakumar, G.O. Hollist, B. Borhan, *Org. Lett.* 5 (2003) 1031–1034.
- [11] S.P. Chavan, S.W. Danatle, C.A. Gavande, M.S. Venkataraman, C. Praveen, *Synlett* 2 (2002) 267–268.
- [12] T.M.A. Shaikh, L. Emmanuvel, A. Sudalai, *Synth. Commun.* 37 (2007) 2641–2646.
- [13] X.F. Wu, C. Darcel, *Eur. J. Org. Chem.* 8 (2009) 1144–1147.
- [14] Y. Diao, R. Yan, S. Zhang, P. Yang, Z. Li, L. Wang, H. Dong, *J. Mol. Catal. A: Chem.* 303 (2009) 35–42.
- [15] K.R. Reddy, M. Venkateshwar, C.U. Maheshwari, S. Prashanthi, *Synth. Commun.* 40 (2010) 186–195.
- [16] J.H. Clark (Ed.), *Chemistry of Waste Minimization*, Chapman & Hall, London, 1995.
- [17] P.T. Anastas, T.C. Williamson (Eds.), *Green Chemistry: Frontiers in Benign Chemical Synthesis and Processes*, Oxford University Press, Oxford, 1998.
- [18] O.V. Zalomaeva, A.B. Sorokin, *New J. Chem.* 30 (2006) 1768–1773.
- [19] E. Kockrick, T. Lescouet, E.V. Kudrik, A.B. Sorokin, D. Farrusseng, *Chem. Commun.* 47 (2011) 1562–1564.
- [20] H. Liu, E. Min, *Green Chem.* 8 (2006) 657–662.
- [21] A.B. Sorokin, E.V. Kudrik, *Catal. Today* 159 (2011) 37–46.
- [22] R.K. Sharma, S. Gulati, S. Sachdeva, *Green Chem. Lett. Rev.* 5 (2012) 83–87.
- [23] R.K. Sharma, C. Sharma, *Tetrahedron Lett.* 51 (2010) 4415–4418.
- [24] A.P. Wight, M.E. Davis, *Chem. Rev.* 102 (2002) 3589–3614.
- [25] C. Li, *Catal. Rev.* 46 (2004) 419–492.
- [26] Q.H. Fan, Y.M. Li, A.S.C. Chan, *Chem. Rev.* 102 (2002) 3385–3466.
- [27] D. Brunel, N. Belloq, P. Sutra, A. Cauvel, M. Lasperas, P. Moreau, F. Di Renzo, A. Galarneau, F. Fajula, *Coord. Chem. Rev.* 1085 (2008) 178–180.
- [28] A. Corma, H. Garcia, *Chem. Rev.* 102 (2002) 3837–3892.
- [29] R. Sharma, S. Dhingra, *Designing and Synthesis of Functionalized Silica Gels and their Applications as Metal Scavengers, Sensors and Catalysts: A Green Chemistry Approach*, LAP Lambert Academic Publishing, Germany, 2011.
- [30] R.K. Sharma, D. Rawat, *Inorg. Chem. Commun.* 17 (2012) 58–63.
- [31] R.K. Sharma, C. Sharma, *J. Mol. Catal. A: Chem.* 332 (2010) 53–58.
- [32] R.K. Sharma, D. Rawat, *J. Inorg. Organomet. Polym.* 20 (2010) 698–705.
- [33] R.K. Sharma, D. Rawat, *J. Inorg. Organomet. Polym.* 21 (2011) 619–626.
- [34] R.K. Sharma, A. Pandey, S. Gulati, *Appl. Catal. A: Gen.* 431–432 (2012) 33–41.
- [35] R.K. Sharma, C. Sharma, *Catal. Commun.* 12 (2011) 327–331.
- [36] R.K. Sharma, D. Rawat, G. Gaba, *Catal. Commun.* 19 (2012) 31–36.
- [37] Z. Biyiklioglu, I. Acar, H. Kantekin, *Inorg. Chem. Commun.* 11 (2008) 630–632.
- [38] T.E. Youssef, *Polyhedron* 29 (2010) 1776–1783.
- [39] A.M. Donia, A.A. Atia, W.A. Al-amrani, A.M. El-Nahas, *J. Hazard. Mater.* 161 (2009) 1544–1550.
- [40] R. Kureshy, I. Ahmad, N.H. Khan, S. Abdi, S. Singh, P. Pandia, R. Jasra, *J. Catal.* 235 (2005) 28–34.
- [41] S. Shylesh, A.P. Singh, *J. Catal.* 228 (2004) 333–346.
- [42] A. Bhatt, K. Pathak, R. Jasra, R. Kureshy, N. Khan, S. Abdi, *J. Mol. Catal. A: Chem.* 244 (2005) 110–117.
- [43] S.B. Hartono, S.Z. Qiao, J. Liu, K. Jack, B.P. Ladewig, Z. Hao, G.Q.M. Lu, *J. Phys. Chem. C* 114 (2010) 8353–8362.
- [44] T. Yokoi, H. Yoshitake, T. Tatsumi, *J. Mater. Chem.* 14 (2004) 951–957.
- [45] M.A.B. Meador, E.F. Fabrizio, F. Ilhan, A. Dass, G. Zhang, P. Vassilaras, J.C. Johnston, N. Leventis, *Chem. Mater.* 17 (2005) 1085–1098.
- [46] S. Shylesh, A.P. Singh, *J. Catal.* 244 (2006) 52–64.
- [47] A.B. Sorokin, P. Buisson, A.C. Pierre, *Mesopor. Micropor. Mater.* 46 (2001) 87–98.
- [48] E. DeOliveira, C.R. Neri, A.O. Ribeiro, V.S. Garcia, L.L. Costa, A.O. Moura, A.G.S. Prado, O.A. Serra, Y. Iamamoto, *J. Colloid Interface Sci.* 323 (2008) 98–104.
- [49] D.J. Upadhyaya, S.D. Samant, *Appl. Catal. A: Gen.* 340 (2008) 42–51.
- [50] C. Pereira, S. Patricio, A.R. Silva, A.L. Magalhaes, A.P. Carvalho, J. Pires, C. Freire, *J. Colloid Interface Sci.* 316 (2007) 570–579.
- [51] A.B. Sorokin, A. Tuel, *Catal. Today* 57 (2000) 45–59.
- [52] H.F. Hoefnagels, D. Wu, G. de With, W. Ming, *Langmuir* 23 (2007) 13158–13163.
- [53] J.-L. Liu, S. Xu, B. Yan, *Colloids Surf. A: Physicochem. Eng. Aspects* 373 (2011) 116–123.
- [54] M. Kruk, M. Jaroniec, Y. Sakamoto, O. Terasaki, R. Ryoo, C.H. Ko, *J. Phys. Chem. B* 104 (2000) 292–301.
- [55] P. Karandhikar, A.J. Chandwadkar, M. Agashe, N.S. Ramgir, S. Sivasanker, *Appl. Catal. A: Gen.* 297 (2006) 220–230.
- [56] F.Z. Su, J. Ni, H. Sun, Y. Cao, H.Y. He, K.N. Fan, *Chem. Eur. J.* 14 (2008) 7131–7135.
- [57] Y. Diaoa, R. Yana, S. Zhanga, P. Yang, Z. Li, L. Wang, H. Dong, *J. Mol. Catal. A: Chem.* 303 (2009) 35–42.
- [58] K.R. Reddy, M. Venkateshwar, C.U. Maheshwari, S. Prashanthi, *Synth. Commun.* 40 (2010) 186–195.
- [59] C. Marsden, E. Taarning, D. Hansen, L. Johansen, S.K. Klitgaard, K. Egeblad, C.H. Christensen, *Green Chem.* 10 (2008) 168–170.
- [60] G. Yin, M. Buchalova, A.M. Danby, C.M. Perkins, D. Kitko, J.D. Carter, W.M. Scheper, D.H. Busch, *Inorg. Chem.* 45 (2006) 3467–3474.